

2D and 3D imaging of ‘tunnel-shaped’ weathering features in soil grains: a biological origin?

Ria L. Mitchell^{1, 2, 3*}, Paul Kenrick², Andrew J. Bodey⁴, James Mansfield⁵, Richard E. Johnston¹

¹Advanced Imaging of Materials (AIM) Core Facility, Faculty of Science and Engineering, Swansea University, Swansea, SA1 8EN, UK (*where work was carried out*)

²Science Group, The Natural History Museum, Cromwell Road, London, SW7 5BD, UK

³ZEISS Microscopy, ZEISS House, 1030 Cambourne Business Park, Cambourne, Cambridge, CB23 6DW, UK (*present address*)

⁴Diamond Light Source, Harwell Science and Innovation Campus, Oxfordshire, UK

⁵Department of Material Science and Engineering, The University of Sheffield, Sir Robert Hadfield Building, Mappin St, Sheffield, S1 3JD, UK

**Corresponding author*: Ria L. Mitchell (ria.mitchell@zeiss.com), Tel: +44(0)1223 401500

ORCID: RLM: 0000-0002-6328-3998; PK 0000-0002-3626-5460; RJ 0000-0003-1977-6418

Keywords: Weathering; X-ray tomography; Synchrotron; Soil; multi-scale 3D imaging

Pre-print statement: At present, this manuscript has not been submitted to a peer reviewed journal and solely exists as a non-peer reviewed EarthArXiv preprint. Please feel free to contact any of the authors, we welcome any feedback.

1. Abstract

The evolution of the first plant-based terrestrial ecosystems some ~450 million years ago had a profound effect on the development of soils and shifts in global biogeochemical cycles, notably drawdown of CO₂ from the atmosphere. In some part these shifts were due to biologically mediated weathering of mineral grains, which until plants evolved, had not been a significant contributor to fluctuations in the Earth system. Here, we investigate modern analogues of the earliest plant-based communities to understand what micro-scale biologically mediated weathering processes might have been occurring in the geologic past. We study analogous organisms such as those in cryptogamic ground covers (CGCs), including bryophyte plants, lichens, fungi, algae, and bacteria. These organisms leave specific markings both externally and internally (e.g., tunnel-like features) in substrates and soil grains, however until now study of these has mostly been limited to two dimensions (2D). We use a combination of non-destructive 3D X-ray microscopy (XRM) and synchrotron X-ray microtomography (sr- μ CT) imaging to characterize potential biologically mediated weathering by a variety of organisms on a range of substrates, including basalt agglomerate proto-soil grains (liverworts, lichen), limestone (lichen), a rhyolite regolith grain (moss, fungi, lichens), and basaltic scoria (mosses, lichen). We conclude that 2D imaging alone can be misleading and a 3D imaging approach must be performed for accurate characterization of tunnel-like features. From initial exploratory scans and observing the data in 2D as ‘digital thin sections’ (slices), we found tunnel-shaped weathering features in three grain examples (agglomerate, limestone, rhyolite regolith), which appear to mostly radiate from grain surface organics. However, once digitally reconstructed and segmented in 3D, those in the agglomerate and rhyolite grains are in fact flattened, lens shaped voids and not singular, tubular tunnels. In contrast, the features in the limestone are more conclusively networks of interconnected tubular shaped tunnels in 3D, while the scoria lacks tunnels but has evidence of larger ‘caverns’ which have developed

beneath grain surface organic material. While it is therefore difficult to interpret these diverse features, particularly the flattened and lens-shaped voids, solely as the result of penetrating biological action (e.g., tubes formed from ‘mining’ fungal hyphae), it is plausible that they could be the result of inorganic dissolution along atomic-scale or chemical boundaries, from organic exudates, or from a combination of the three. The identification, careful morphological characterization, and cautious interpretation of these features has implications not only for understanding how the earliest terrestrial soil biotas weathered their substrates here on Earth, but also for understanding similar features, potentially inferred as biological in origin, in highly topical extra-terrestrial rocks (e.g., on Mars), and in engineering applications where the presence of such features may be detrimental (e.g., to nuclear waste glass durability).

2. Introduction

When plants and other associated organisms first extensively colonised terrestrial landscapes in the early Palaeozoic (450-500 Ma; Morris et al., 2018, Puttick et al., 2018, Strother and Foster, 2021) as cryptogamic ground covers (CGCs; Elbert et al., 2012; Edwards et al., 2015; Mitchell et al., 2016), they had an influential effect on the Earth system. This included shifts in the evolution and architecture of fluvial sedimentary systems through diverse stabilization strategies (Gibling and Davies, 2012; McMahon and Davies, 2018; Mitchell et al., 2023), soil development (Mitchell et al., 2021a; Mergalov et al., 2018), weathering (Field et al., 2012; Lenton et al., 2012), and atmospheric CO₂ drawdown; the latter being partly due to weathering, but also partly due to increased burial of organic carbon from significantly greater and more extensive plant biomass (Field et al., 2016; Mills et al., 2017; Porada et al., 2014; Elbert et al., 2012; Berner and Kothavala, 2001). Modern analogous examples of CGCs, which are varied communities of bryophyte plants (liverworts, hornworts, and mosses), fungi,

cyanobacteria, lichens, and algae, can be studied to understand some of the weathering features contained within the soil and on individual soil grains, enabling elucidation of the micro-to-nano scale weathering processes which lead to large-scale atmospheric and environmental change. It is thought that symbionts (such as mycorrhizal fungi) were partly responsible for the biologically mediated weathering which led to CO₂ drawdown because of targeted elemental (nutrient) acquisition from minerals (i.e. through ‘mining’ of essential elements in a reciprocal symbiotic relationship; Field et al., 2012; Lenton et al., 2012; Lenton et al., 2017), however no in-situ fossil evidence of the interactions between soils and symbionts, where both the plant and soil components are preserved together, exists in the rock record to elaborate on these sorts of relationships. From studying modern analogues, many surficial and internal biologically mediated weathering features (BMFs; Mitchell et al., 2019) exist, including internal tunnels, which have been inferred as biological in origin. Tunnels have also been discovered from both field and laboratory studies of modern CGC organisms, specifically fungal hyphae and bacteria, and attributed to a biological source, whether that be directly (biomechanical forcing and ‘mining’), or indirectly (secretion, exudate and root-mediated dissolution) (Mitchell et al., 2019; Furnes et al., 2007; McLoughlin et al., 2009, 2010; Landeweert et al., 2001; van Scholl et al., 2008, Jongmans et al., 1997; Hoffland et al., 2002; Thorseth et al., 1995; Thorseth et al., 2001). However, most of these studies are from a 2D perspective using optical microscopy, scanning electron microscopy, etc, with a handful of 3D studies showing the complete structure, shape and morphology of the tunnels (Mitchell et al., 2021b; Ivarsson et al., 2018).

Here, we use a combination of non-destructive 3D X-ray microscopy (XRM) and synchrotron X-ray microtomography imaging (sr μ CT) to investigate tunnel-like weathering features. We also employ a multi-scale imaging approach to improve resolution at smaller fields of view. We investigate four substrates, three volcanic (basaltic agglomerate, scoria, rhyolite regolith) and one carbonate (limestone), hosting various communities of living CGCs.

We use initial exploratory scans and observe the data in 2D as ‘digital thin sections’ (slices) to search for potential tunnel-shaped weathering features, and then segment and visualise the data in 3D to establish if various features (shape, size, organic material content) are consistent with the biologically-derived tunnel hypothesis. Our aim is to understand how features like these can shed light on how organisms in the geologic past contributed to weathering in early terrestrial ecosystems and the formation of proto-soils (e.g., Mitchell et al., 2021), and what features we need to search for in the rock record to identify these interactions (e.g., Mitchell et al., 2019). This work also has implications for understanding the causes of weathering features observed in extra-terrestrial rocks (e.g., on Mars) in future sample return to Earth missions, and, from a modern engineering perspective, specifically in the dissolution of borosilicate glasses used in nuclear waste containment (Mansfield, 2022).

3. Materials and Methods

3.1. Samples and field locations

Grain and rock samples were collected within cryptogamic ground cover (CGCs) soil cores from Iceland (agglomerate soil grain, scoria), Wales (limestone) and New Zealand (rhyolite soil grain) (Table 1). Grains were extracted by picking from proto-soil cores using a light microscope and tweezers. X-ray Microscopy (XRM) samples were glued to the end of cocktail sticks using glue gun adhesive, whilst synchrotron grain samples were attached with a cyanoacrylate-based superglue to the end of steel pins. Cocktail sticks and pins were then mounted in sample holders for the respective instruments.

	Agglomerate grain	Limestone	Rhyolite grain	Scoria
Dominant chemistry	Basalt - Mg, Fe, Ca rich	Limestone - CaCO ₃	Rhyolite-like – Si, K, Na, Al rich	Basalt – Mg, Fe, Ca rich
Grain phases?	Yes – two, based on density differences	Homogeneous	Yes – mostly homogeneous, but with limited high density minerals	Yes - many
Environment	Subsurface soil grain	Rocky outcrop	Surface soil grain	Surface soil grain
Plants or other organisms?	Sampled from within liverwort CGC proto-soil	Sampled with lichen growing directly on it	Sampled from surface of mixed moss and lichen CGC proto-soil	Sampled from surface of mixed moss and lichen CGC proto-soil
Provenance	Iceland	Wales	New Zealand	Iceland
Features	Grain containing few large tunnel-shaped features	Rock containing many small tunnel-shaped features	Grain containing few large tunnel-shaped features	‘Caverns’ below organic material
Organics imaged?	Yes, filamentous bundles surrounding grain surface, possibly inside tunnel-shaped features	Yes, lichen growing directly on surface of rock	Possibly unidentified crusts on grain surface, possibly inside tunnel-shaped features	Yes, moss and lichen growing directly on grain surface
Technique used	Laboratory-based XRM	Laboratory-based XRM	Synchrotron	Laboratory-based XRM
Multi-scale?	Yes	Yes	No	Yes

Table 1: Description of samples used in this study

3.2. Laboratory-based X-ray Microscopy (XRM)

A ZEISS Xradia Versa 520 (Carl Zeiss Microscopy, Pleasanton, CA, USA) X-ray Microscope (XRM) was used to carry out laboratory-based high resolution non-destructive 3D tomographic imaging. The set up includes a CCD detector system with scintillator-coupled visible light optics and a tungsten transmission target. Initial low resolution (large field of view) scans were performed on the subsurface soil grain and the lichen limestone followed by successively higher resolution (smaller field of view) targeted scans via the Scout and Zoom approach (Figure 1). Multi-scale scans of the agglomerate soil grain were achieved using an X-ray tube voltage ranging between 80 and 110 kV, a tube current of 87 and 91 μA , and an exposure time of 1 to 32 seconds. A total of 3201 projections were collected for each scan. A filter (LE5) was used to filter out unwanted lower energy X-rays on the highest resolution scan, and the 0.4x, 4x and 20x objective lenses were selected with binning set to 2, producing isotropic voxel (3D pixel) sizes ranging between 4.94 and 0.47 μm (Figure 1 c). Multi-scale scans of the lichen limestone were also achieved at X-ray tube voltages ranging between 80 and 110 kV, a tube current of between 87 and 91 μA , and exposure times of 1 to 27 seconds. A total of 3201 projections were collected for each scan. No filtering was necessary for these scans. The 0.4x and 4x objective lenses were selected with binning set to 2, producing isotropic voxel (3D pixel) sizes ranging between 7.17 and 0.24 μm (Figure 1 c). Scan times for all scans ranged between 2 and 26 hours. The tomograms were reconstructed from 2D projections using a ZEISS Microscopy commercial software package (XMReconstructor), and an automatically generated cone-beam reconstruction algorithm based on filtered back-projection. These scans were obtained within the Advanced Imaging of Materials (AIM) Core Facility at Swansea University, UK, and multi-scale scans were correlated using ORS Dragonfly software.

3.3. Synchrotron X-ray microtomography (sr- μ CT)

Synchrotron tomography was performed at the Diamond-Manchester Imaging Beamline I13-2 at Diamond Light Source synchrotron (Oxfordshire, UK) for high throughput, high flux scanning. A partially-coherent and near parallel polychromatic pink beam was generated from an undulator in an electron storage ring at 3.0 GeV and 300 mA current. The scans were achieved at 23 kV using the 2x objective, resulting in a 1.625 μ m voxel size, and were collected using a 0.045 step size at 0.09 seconds exposure time. The sample, at 10 mm propagation, was rotated 180°, and 4001 projections were collected. A pco. Edge 5.5 camera link (PCO AG, Kelheim, Germany) detector consisting of 2560 x 2160 pixels was used to collect images, resulting in scan times of 2 to 4 minutes. Data was reconstructed using a filtered back projection algorithm within Savu software.

ZEISS ZEN Intellesis machine learning software was used to segment the features of interest in 3D for all scans. All XRM and synchrotron data were rendered and visualised using a mixture of ORS Dragonfly and Thermo Fisher Scientific Avizo software. Both laboratory-based and synchrotron-based scans were collected due to ease of accessibility and collection of multi-scale scans in the laboratory, and the speed of scans at the synchrotron.

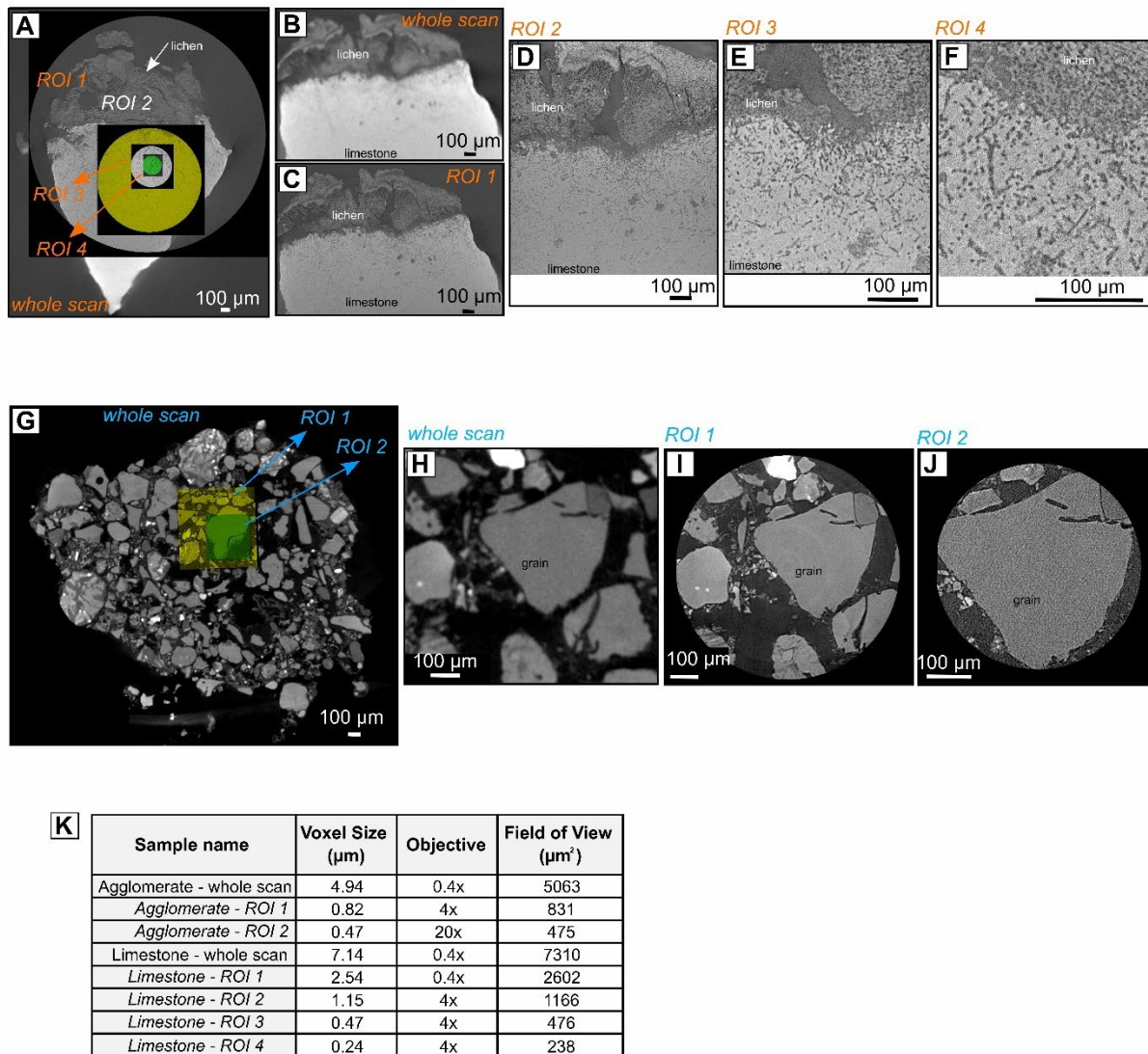


Figure 1: Multi-scale 3D XRM scans using ZEISS Microscopy Scout and Zoom, showing the locations of higher resolution region of interest (ROI) scans. A-F: Multi-scale scans for the limestone. G-J: Multi-scale scans for agglomerate grain. K: Table showing variations in voxel size, objective and field of view size for each ROI scan; note improvement in scan quality with successively higher resolution scans (c, e, f, h-j).

3. Results and Discussion

3.1 Multi-scale and multi-dimensional 3D imaging

3D X-ray imaging has the advantage over other techniques because of the ability to study samples non-destructively in both 2D as ‘digital thin sections’ (from individually reconstructed tomograms) and in 3D (as a reconstructed volume). 3D volumes generated from X-ray imaging can be composed of a series of 2D ‘slices’ (tomograms), usually as a .tiff stack. The individual slices enable the viewing of internal data as ‘2D digital thin sections’ without the need to cut or destroy the sample, as is the case with traditional $\sim 30\ \mu\text{m}$ thick glass-mounted thin sections, commonly used in the geological sciences to view ‘inside’ samples. Moreover, multi-scale 3D imaging provides a novel means of examining the same sample at different fields of view, spatial resolutions, and voxel (3D pixel) sizes, providing improving levels of detail of one sample with subsequent region of interest (ROI) scans at higher resolution (Figure 1). The Scout and Zoom feature of the ZEISS Microscopy Versa series laboratory-based X-ray microscopes enables multi-scale study within the same regions of interest using a series of different objective lenses, enabling the correlation of data at different scales. This is particularly useful for the study of weathering features in soil grains as it enables targeted areas (i.e., tunnel features) to be studied, which are likely to not be detected until an initial, low resolution exploratory scan, and can be further scrutinised with higher resolution scans. While we have not conducted a full correlative imaging investigation in this study, other work exists (e.g., Mitchell et al., 2021b) which has the advantage of investigating soil grain weathering features across scales, dimensions, and modes, with the combination of imaging data with chemical data.

3.2 Weathering features in 2D vs 3D

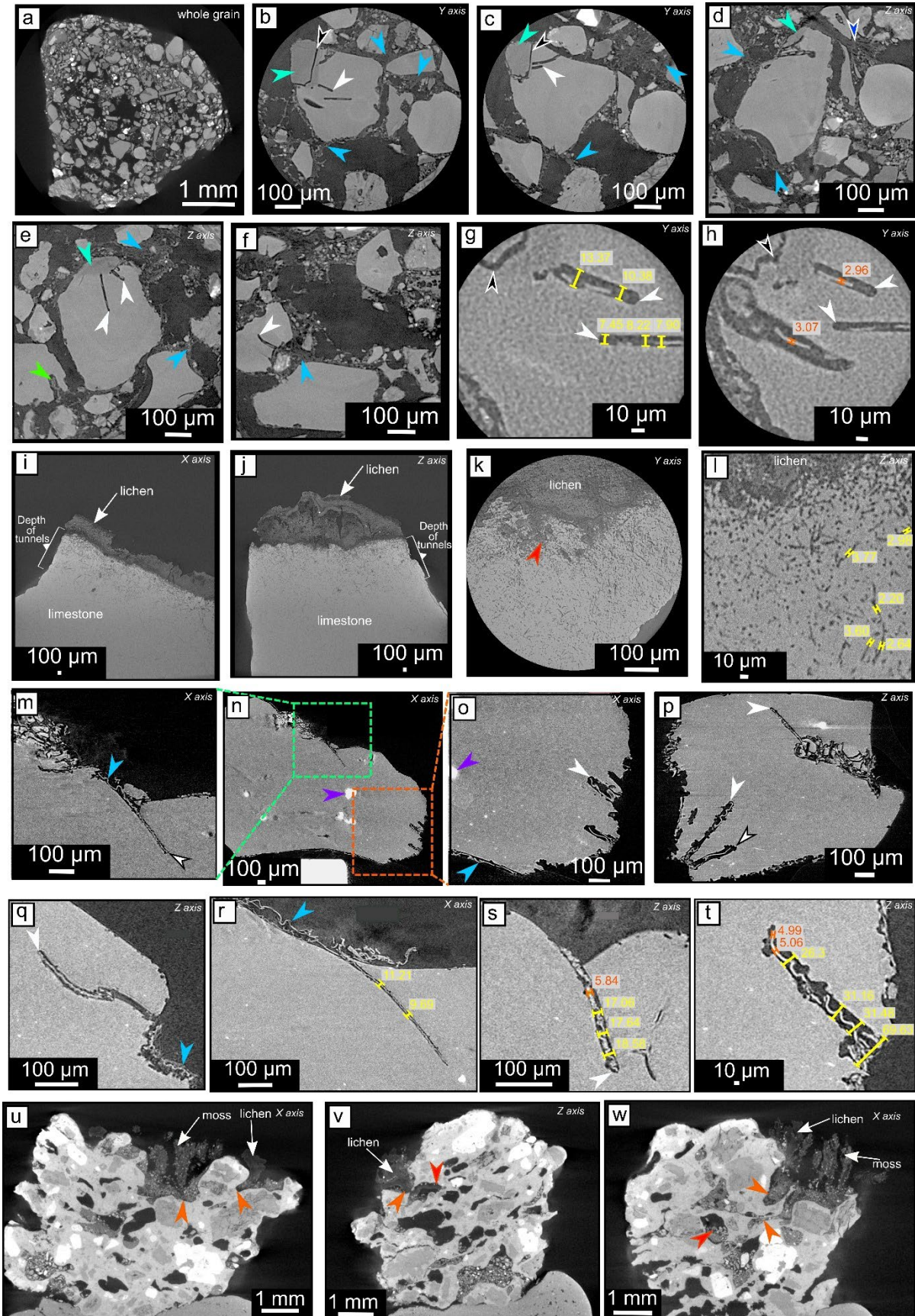


Figure 2: 2D slice views, or ‘digital thin sections’, of agglomerate soil grain (a-h), limestone (i-l), rhyolite grain (m-t), and scoria (u-w). A: Slice showing that the subsurface soil grain is composed of numerous smaller grains. B-E: 2D features associated with the grain of interest including internal elongate tunnels with rounded tips (white arrow) that often contain organic-like filamentous structures, larger tunnels containing organics (green arrow), darker, lower density areas of the grain with a presumed different chemical composition (turquoise arrow), and external organic material (light blue arrow) which often forms tubular cyanobacterial-like bundles (dark blue arrow). Cracks are also noted (black arrow) that are morphologically different to tunnels. G-H: Measurements indicate tunnels are between 7.4 and 13.4 μm wide, and filamentous organic-like structures within the tunnels are up to 3.1 μm wide. I-L: 2D features associated with lichen limestone indicate networks of multi-directional tubular tunnels which extend ~ 3 mm into the limestone. Endolithic lichen communities also appear to be present (red arrow). Tunnels appear to be up to 3.8 μm wide. M-T: 2D features associated with the rhyolite grain include diverse elongate grain tunnels with rounded tips (white arrow) which often contain filamentous organic material extending from the grain surface (blue arrow). Some tips have flat ends (white arrow with black outline). High density grain minerals also seen (purple arrow). Tunnel width varies between 9.7 and up to 69.6 μm at tunnel openings at the grain surface, whereas internal filamentous structures range between 5 and 5.8 μm width. U-W: 2D features associated with scoria grain. No tunnels are observed, but caverns have developed beneath moss and lichen surface communities (orange arrow) which appear to contain endolithic communities (red arrow).

Using the ‘digital thin section’ approach, we are able to observe various tunnel-shaped features from the 2D slices in our four samples (Figures 1-2), and later render them in 3D.

In the subsurface agglomerate soil grain, elongate tunnel-shaped features with rounded tips are observed (Figure 2 a-h) in one grain. These appear to originate from the outside of the soil grain (Figures 2 b-f), and are of various widths ranging from 7.45 to 13.37 μm (Figure 2 g). Surrounding the soil grain, there also appears to be organic material resembling tubular,

cyanobacterial-like bundles (Figures 2 b-f) which could be holding some of the grains within the agglomerate, and some larger tunnel-shaped features appear to contain organic material (Figure 2 e). There are other features, possibly resembling filaments or weathering rinds, contained within some of the tunnels that range in width from 2.96 to 3.07 μm (Figure 2h). What look like mechanical cracks are also present within this grain (Figures 2 b, c, g, h), having a different shape, roundness and smoothness compared to the tunnel-shaped features. Additionally, there are different chemical phases in this grain, represented by differing X-ray attenuation grayscales (Figures 2 b-e); while we cannot quantify the chemical composition from the imaging undertaken here, we are able to identify that greyscale differences relate to the density differences of the composing minerals/phases, which in turn are related to their elemental constituent z-numbers. The mechanical crack seems to only be contained in the darker (less dense) chemical phase, and no tunnel-shaped features are located here either (Figures 2 b-e). This is supported by viewing the grain in 3D (Figure 3 a-d), where no tunnel shaped features appear to be present in this region. This could be a function of the chemical composition of this darker phase of the grain, where dissolution might be less likely to occur due to the elemental composition. Unlike the 2D tiffs, the 3D rendering suggests that the tunnel-shaped features originate from the mechanical crack (Figure 3 b), and, importantly, that the features are not in fact tunnel shaped but form flattened, lens shaped voids (Figures 3 a-d). 3D rendering indicates that they extend from a central 'spine', and the whole network is almost corkscrew in shape (Figures 3 a-d). There are however some smaller, straight, tube shaped features, but these are restricted to the few millimetres beneath the surface of the grain (Figures 3 c-d).

In the lichen-hosting limestone, there are numerous diverse networks of individual tunnel-shaped features (Figure 2 i-l) which appear to be multi-directional and extend to ~ 3 mm depth in the limestone (Figure 2 i-j). Using the highest resolution scan, the tunnel-shaped

features appear to be between 2.20 and 3.77 μm wide, so smaller than those found in the agglomerate soil grain. There also appears to be endolithic lichen communities in the subsurface of the limestone (Figure 2 k). This sample really benefitted from multi-scale X-ray imaging to be able to see the tunnel-shaped features in greater detail. Once rendered in 3D, it is clear that these concur with the 2D data and are tunnel shaped, rather than lens shaped voids in the agglomerate grain. The tunnel networks have been digitally segmented and analysed, showing that many of the tunnels are joined to form individual, interconnected networks (Figure 3 g). There is also variation in their directionality so not all tunnels develop downwards away from the surface lichen layer (Figure 3 h), and there is variation in the thickness of the tunnel networks from 3 to 54 μm (Figure 3 i).

A rhyolitic regolith grain also contains tunnel-shaped features which are very similar to those found in the agglomerate soil grain (Figures 2 m-t). These are elongate features, sometimes with rounded tips (Figures 2 o, p, q, s) but sometimes with wedge-shaped tips (Figure 2 p). The tunnel-shaped features are up to 69.63 μm in width at their openings on the outside of the grain, and range between 31.48 and 9.69 μm through their length. Some of the tunnel-shaped features appear to originate from organic-like crusts on the surface on the grain (Figures 2 m, o, q, r), with some features appearing to contain organic-like filaments (Figures 2 m-t), which range in width from 4.99 to 5.84 μm . Once rendered in 3D, some of the tunnel-shaped features however form flattened, lens-shaped voids with some others near surface forming more elongate, tube-like structures (Figures 3 j-m), very similar to those in the agglomerate soil grain. Many of the tunnel shaped features appear to be associated with (or near to) the higher density minerals located in this sample (Figures 3 l-m), suggesting that these tunnels may be remnants of their weathering.

In the scoria grain, which hosts communities of lichens and moss, numerous ‘caverns’ have developed beneath the growing surface organic material (Figures 2 u-w). These caverns

do not appear to develop as singular, tubular tunnels as in the other examples, but rather wider weathering features often containing endolithic communities and inorganic detritus. These likely originate from weathering by endolithic communities within vesicles and pores, as this sample appears much more porous compared to the others.

From these observations we deduce that a) it is important to supplement 2D imaging results and interpretations with 3D imaging data which paints a clear picture of the real interconnected nature of the structures, and b) that it could be useful to use multiple techniques (or at least, imaging at the multi-scale) in combination, e.g., in a correlative imaging and characterisation workflow.

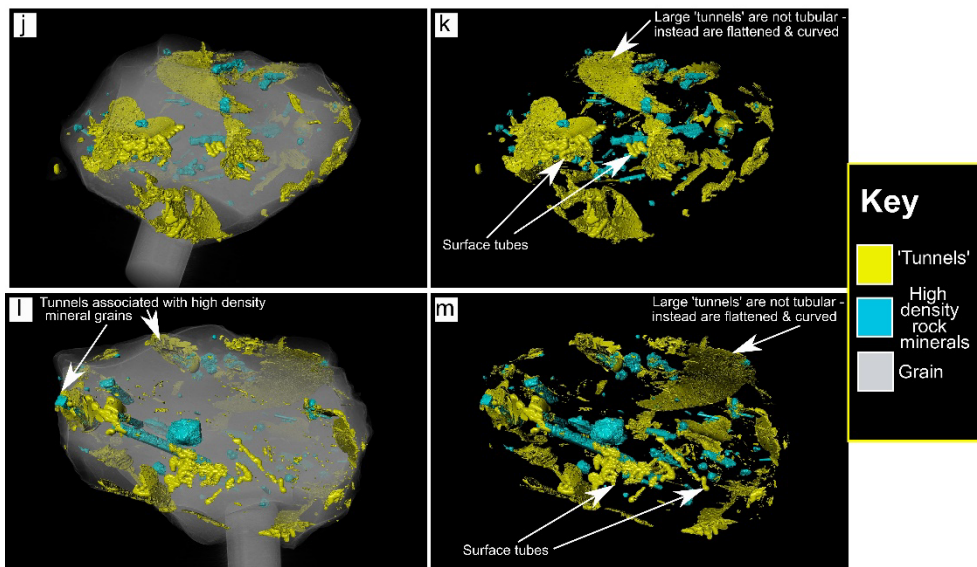
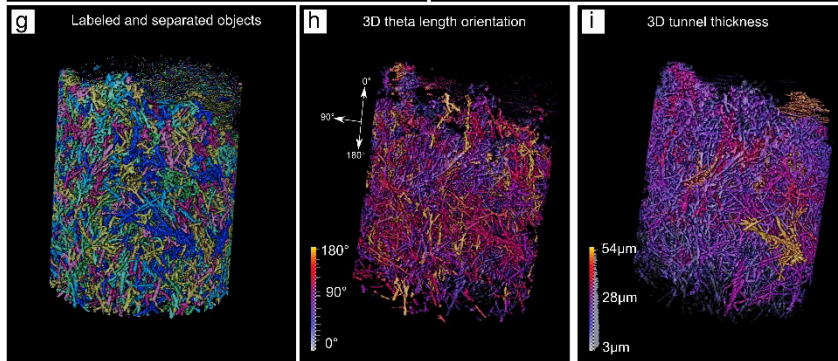
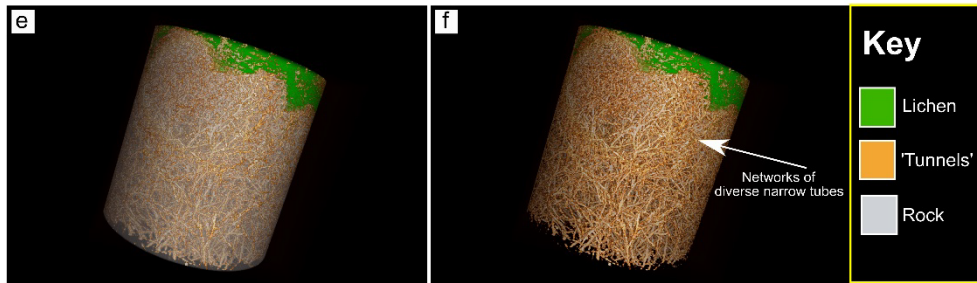
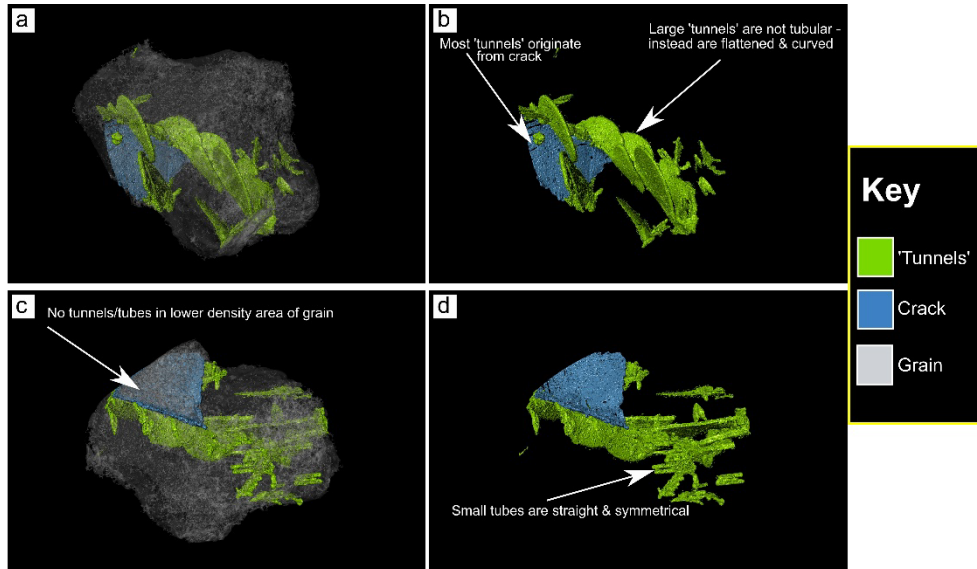


Figure 3: 3D views of segmented grain features in agglomerate soil grain (A-D), lichen limestone (E-I), and rhyolite regolith grain (J-M). A-D: 3D segmentation reveals the subsurface tunnels are not tubular, but instead flattened and curved, mostly extending from a central ‘spine’. Some straight tubular tunnels are present near the surface. Crack segmentation around the lower density area of the grain reveals a lack of tunnels within this area of the grain. E-F: 3D segmentation of diverse tubular tunnel networks in lichen limestone. Analysis of the tubular tunnels reveals many joined tunnels networks (g) that have variety in their length orientation from the sample surface (h) and also in their thickness (i). J-M: 3D segmentation reveals subsurface tunnels are again not tubular, but form flattened and curved structures. Some tubular structures exist near the grain surface. Many subsurface tunnels are associated with high density mineral grains (l) indicating that they may be prone to weathering.

3.3 Caused by biology?

In this study, we have shown that some 2D observations consistent with potentially biologically mediated tunnel-shaped features are in fact flattened, lens shaped voids when visualised in 3D. This casts doubt on their solely biological origin.

2D tunnel-like features have been identified and extensively discussed in the literature, and have had their formation and occurrence mostly attributed to a biological origin (Furnes et al., 2007; McLoughlin et al., 2009, 2010; Berner and Cochran, 1998; Landeweert et al., 2001; van Scholl et al., 2008, Jongmans et al., 1997; Hoffland et al., 2002; Ivarsson et al., 2018; Thorseth et al., 2001). These examples are mostly justified because of the presence of other proximal biological factors, or indeed the presence of organic material within the tunnel features. Despite this, these studies could benefit from complementary 3D imaging to add weight to their interpretations. Symbiotic fungal hyphae are known to create such tunnel (as well as other surficial) features through a combination of nanometre-scale biomechanical forcing and acidic dissolution from the excretion of low molecular weight organic anions

(LMWOAs, e.g. oxalate), phosphoric acids, protons, and extracellular polymeric substances (EPS) (Hoffland et al. 2004; Bonneville et al. 2009; Pinzari et al., 2021; Bray et al., 2015; Rosling et al., 2004; Gadd 2007, 2010), which promotes dissolution and mobilizes specific elements (e.g. Mg, Ca, K) and cations (Landeweert et al. 2001; Bonneville et al. 2009) from the grain to the host organism. A particular example attributes fungi for up to 16% of the weathering of olivine in an Mg deficient forest soil (Wild et al., 2021). A criteria has been developed to identify such features attributed to a fungal origin: this includes them having smooth sides, rounded tips, and constant diameters (e.g., Ivarsson et al., 2018, McLoughlin et al., 2009; Hoffland et al., 2002); they're usually straight and sometimes funnel shaped (Ivarsson et al., 2018); and sometimes ramified (Landeweert et al., 2001). All of these shapes being retained after the hypha degrades. Conversely, there are other tunnel-like features which are less clearly singularly attributed to a biological origin in the literature (e.g., Dultz et al., 2014; Kruber et al., 2008; Mitchell et al., 2021), and there are also examples of features which meet the above biological criteria but which were produced abiotically via laboratory-based alteration experiments of both natural analogue and synthetic glasses (Fisk et al., 2013; Fisher, 2020; Mann et al., 2019; Backhouse, 2007; Mansfield, 2022). Other examples exist that are due to chemical and/or pressure dissolution (McLoughlin et al., 2010), and others attributed to ambient inclusion trails (AITs). At first glance AITs very much resemble biologically-mediated tunnels, however they are most likely an abiotic product of mineral grains propelling through substrate, leaving a terminal grain at the end of the tunnel (Wacey et al., 2008; McLoughlin et al., 2010). This however is something we do not observe in the samples in this study and so can be discounted. Burial metamorphism of biological matter can also generate morphologically similar features (Lepot et al. 2011).

All of these examples of causes (biotic, a mixture, abiotic) have specific features in common with the 2D examples presented in this study; this includes smooth-sided tunnels,

rounded tips, wedge-shaped tips, smaller tunnels on grain surfaces (which look remarkably like those in Dultz et al., 2014), material inside the tunnels (which are probably likely to be alteration rinds; Thorseth et al., 2001), and that they originate from organic/biologically-rich areas on the outside of the grain. We propose that the tunnel-shaped features described in this study could be due to a mixture of both biotic and abiotic processes, with the contact of the external/surficial biological component the driver of the weathering, similar to the tunnel features described in Mitchell et al., 2021b. While the 2D results may convincingly (and erroneously) be attributed to a solely biological origin, the flattened, lens shaped voids identified in 3D don't, and likely a) originate along weaknesses in the atomic structure/cracks/crystal boundaries/mineral boundaries within the same grain (e.g., Backhouse, 2007), and/or b) from in-situ secretion of organic acids and other exudates from the surrounding organic material, leading to the irregular (non-straight) shape of the voids (e.g., as in Mitchell et al., 2021b). The latter seems particularly likely in the basalt and rhyolite examples as both grains are surrounded by filamentous organic material, and so are, at least in part, likely due to secretion of organic acids and exudates (which are known to alter rock surfaces; Zaharescu et al., 2020). As discussed in Mitchell et al., (2021b), another possibility is that the voids could also have developed from CO₂ enriched soil water creating abiotic chemical dissolution, which could be exacerbated by below-ground biological respiration of CO₂ and exudates from microbes could indirectly be responsible for mineral attack and dissolution.

The chemistry of the containing grain and/or substrate will also have an effect on how easily/difficult it will weather. Indeed, fungi are reported to have varying levels of weathering intensity which can be based on the production of oxalic acid, a secretion which can be adapted and modified to the chemistry of the minerals it comes into contact with (Pinzarri et al., 2016, 2021; Schmalenberger et al., 2015). Basalts and limestones will generally weather more readily, and in the basalt this is likely due to the high proportion of feldspars which are more

prone to chemical attack (Mitchell et al., 2021b). Further, the presence of feldspars might actually increase their susceptibility for chemical attack (Berner and Chochrain, 1998; Landeweert et al., 2001). The limestone is perhaps even more prone to chemical attack, and can be subject to dissolution from simple rainwater. The tubular structure of the tunnel-shaped features in the limestone though, in contrast to the flattened, lens shaped voids in the basalt and rhyolite examples, suggests that there is potentially a more ordered, biological influence on this sample. While we cannot observe any organic material inside the tunnels themselves and rule out an entirely abiotic influence, that does not mean that they aren't there, and they could be out of the resolution range of the laboratory based XRM. The shape and size of these are consistent with tunnels associated with fungal hyphae which will scavenge the grain/rock for mineral nutrients while cyanobacteria will confine themselves to lichen surfaces because of the need to photosynthesise.

Our results show that it is possible to misinterpret possible biological-like weathering features when studying only in 2D. This has implications not only for understanding the biological impact on weathering in the geologic past on Earth, but also for understanding similar features, potentially being inferred as biological in origin, in future sample return missions of extra-terrestrial rocks (e.g., on Mars). Recently, this has been the focus of topical debate in the literature (e.g., McMahon and Cosmidis, 2021; Bosak et al., 2021; Steele et al., 2022), with a suggested drive for better understanding of not only biological influences on biosignatures and bioweathering, but also abiotic influences, so a criteria can be laid out to differentiate between them. This will not only elucidate potential features in the geologic past, but also in the search for life on extra-terrestrial planets and bodies. While it is important to differentiate between biotic and abiotic (or a mixture of the two), results presented here suggest it is also important to examine findings in multiple dimensions, allowing for a complete narrative, from an imaging perspective, to be achieved. Further imaging and analysis of in-situ

weathering experiments could take this one step further by combining data from multi-dimensional, multi-modal, and multi-scale techniques in a correlative imaging workflow (e.g., Mitchell et al., 2021b).

Conclusions

We are able to observe various tunnel-shaped features from ‘digital thin sections’ as 2D slices in our four samples, however, these features look very different once rendered and visualised in 3D. Therefore, care must be taken when interpreting 2D tunnel-shaped weathering features, whether they are identified from 3D X-ray imaging, scanning electron microscopy (SEM), optical microscopy (OM), from glass-mounted thin sections, or other 2D imaging techniques. Time resolved (i.e. 4D) experiments are needed to better understand how these features form under various scenarios (with or without biological communities of different compositions, solutes of differing chemistries, grains/rocks of different mineralogies and chemical makeup, etc) to elucidate the exact cause of these tunnel- and lens-shaped features. Once that is established, greater confidence can be put to identifying similar features not only in the geologic past, but also in extra-terrestrial environments, where the search for bio-geo interactions is particularly significant.

Acknowledgements

Authors acknowledge AIM Facility funding in part from EPSRC (EP/M028267/1), the European Regional Development Fund through the Welsh Government (80708), the Ser Solar project via Welsh Government, and from Carl Zeiss Microscopy. Thanks also goes to DLS for beamtime at I13-2 under proposal MG21506, and to Jebin Jestine, James Russell, Sarah Aldridge and Alan Spencer for beamtime shift assistance.

References

- Backhouse D. J. 2017. A study of the dissolution of nuclear waste glasses in highly-alkaline condition.s PhD thesis, The University of Sheffield. <http://etheses.whiterose.ac.uk/16760/>
- Berner, R. A., and Kothavala, Z. 2001. GEOCARB III: A Revised Model of Atmospheric CO₂ over Phanerozoic Time, *American Journal of Science*, v. 301, p. 182-204, Doi: 10.2475/ajs.301.2.182.
- Berner, R. A., Cochran, M. F. 1998. Plant-induced weathering of Hawaiian basalts. *J. Sediment. Res.* v. **68**, 723–726.
- Bonneville, S., Smits, M. M., Brown, A., Harrington, J., Leake, J. R., Brydson, R., and Benning, L. G. 2009. Plant-driven fungal weathering: Early stages of mineral alteration at the nanometer scale, *Geology*, v. 37, p. 615-618.
- Bosak, T., Moore, K.R., Gong, J. et al. 2021. Searching for biosignatures in sedimentary rocks from early Earth and Mars. *Nat Rev Earth Environ* **2**, 490–506.
<https://doi.org/10.1038/s43017-021-00169-5>
- Bray AW, Oelkers EH, Bonneville S, Wolff-Boenisch D, Potts NJ, Fones GR, Benning LG. 2015. The effect of pH, grain size, and organic ligands on biotite weathering rates. *Geochim Cosmochim Acta.* 164, p. 127–145. DOI: 10.1016/j.gca.2015.04.048
- Dultz, S., Boy, J., Dupont, C., Halisch, M., Behrens, H., Welsch, A. M., Erdmann, M., Cramm, S., Hlesch, G., Deubener, J. 2014. Alteration of a Submarine Basaltic Glass under Environmental Conditions Conducive for Microorganisms: Growth Patterns of the Microbial Community and Mechanism of Palagonite Formation. *Geomicrobiology*, v. 31, issue 9, p. 813-834, DOI: 10.1080/01490451.2014.89774.

Edwards, D., Cherns, L., & Raven, J. A. 2015. Could land-based early photosynthesizing ecosystems have bioengineered the planet in mid-Palaeozoic times? *Palaeontology*, v. 58, p. 803–83. DOI: 10.1111/pala.12187

Elbert, W., Weber, B., Burrows, S., Steinkamp, J., Büdel, B., Andreae, M. O., Pöschl, U. 2012. Contribution of cryptogamic covers to the global cycles of carbon and nitrogen. *Nature Geoscience*, v. 5, p. 459–462. DOI: 10.1038/ngeo1486

Field, K. J., Rimington, W. R., Bidartondo, M. I., Allinson, K. E., Beerling, D. J., Cameron, D. D., Duckett, J. G., Leake, J. R., Pressel, S. 2016. Functional analysis of liverworts in dual symbiosis with Glomeromycota and Mucoromycotina fungi under a simulated Palaeozoic CO₂ decline. *ISME Journal*, v. 10, p. 1514–1526. DOI: 10.1038/ismej.2015.204

Field, K. J., Cameron, D. D., Leake, J. R., Tille, S., Bidartondo, M. I., & Beerling, D. J. 2012. Contrasting arbuscular mycorrhizal responses of vascular and non-vascular plants to a simulated Palaeozoic CO₂ decline. *Nature Communications*, v. 3, p. 1–8. DOI: 10.1038/ncomms1831

Fisher, A. J. 2020. *Dissolution of UK Vitrified High-Level Radioactive Waste Containing Zinc and Calcium*. PhD thesis, The University of Sheffield.

Fisk, M. R., Crovisier, J. L., Honnorez, J. 2013. Experimental abiotic alteration of igneous and manufactured glasses. *Comptes Rendus Geoscience*, v. 345, is. 4, p. 176-184, DOI: 10.1016/j.crte.2013.02.001.

Furnes, H., Banerjee, N. R., Staudigel, H., Muehlenbachs, K., McLoughlin, N., Wit, M., Van Kranendonk, M. 2007. Comparing petrographic signatures of bioalteration in recent to Mesoarchean pillow lavas: Tracing subsurface life in oceanic igneous rocks. *Precambrian Research*, v. 158, p. 156-176.

Gadd, G. M. 2010. Metals, minerals and microbes: geomicrobiology and bioremediation. *Microbiology*, v. 156, p. 609–643.

Gadd, G. M. 2007. Geomycology: biogeochemical transformations of rocks, minerals, metals and radionuclides by fungi, bioweathering and bioremediation. *Mycol. Res.*, v. 111, p. 3-49.

Gibling, M. R., Davies, N. S. 2012. Palaeozoic landscapes shaped by plant evolution. *Nature Geoscience*, v. 5, p. 99–105. DOI: 10.1038/ngeo1376

Hoffland, E., Kuyper, T. W., Wallander, H., Plassard, C., Gorbushina, A. A., Haselwandter, K., Holmström, S. et al. 2004. The Role of Fungi in Weathering. *Frontiers in Ecology and the Environment* v. 2, no. 5, p. 258–64. DOI: 10.2307/3868266.

Hoffland, E., Giesler, R., Jongmans, T. & Van Breemen, N. 2002. Increasing feldspar tunneling by fungi across a North Sweden podzol chronosequence. *Ecosystems* v. 5, p. 11–22.

Ivarsson, M. et al. 2018. Intricate tunnels in garnets from soils and river sediments in Thailand-Possible endolithic microborings. *PLoS ONE* v. 13, 0200351.

Jongmans, A., van Breemen, N., Lundström, U. et al. 1997 Rock-eating fungi. *Nature* v. 389, p. 682–683. [DOI:10.1038/39493](https://doi.org/10.1038/39493)

Kruber, C., Thorseth, I. H., and Pedersen, R. B. 2008. Seafloor alteration of basaltic glass: Textures, geochemistry, and endolithic microorganisms. *Geochem. Geophys. Geosyst.*, v. 9, Q12002, DOI:10.1029/2008GC002119.

Landeweert, R., Hoffland, E., Finlay, R. D., Kuyper, T. W. & Van Breemen, N. 2001. Linking plants to rocks: Ectomycorrhizal fungi mobilize nutrients from minerals. *Trends Ecol. Evol.* v. 16, p. 248–254.

Lepot, K., Benzerara, K., Philippot, P. 2011. Biogenic versus metamorphic origins of diverse microtubes in 2.7 Gyr old volcanic ashes: Multi-scale investigations. *Earth and Planetary Science Letters*. v. 312, is. 1-2, p. 37-47. DOI: 10.1016/j.epsl.2011.10.016

Lenton, T. M., Krause, A. J., Shields, G. A., Scotese, C. R., Hill, D. J., Mills, B. J. W. 2018. Modelling the long-term carbon cycle, atmospheric CO₂, and Earth surface temperature from late Neoproterozoic to present day. *Gondwana Research*, v. 67, p. 172–186.

Lenton, T. M., Crouch, M., Johnson, M., Pires, N., Dolan, L. 2012. First plants cooled the Ordovician. *Nature Geoscience*, v. 5, p. 86–89. [DOI: 10.1038/ngeo1390](https://doi.org/10.1038/ngeo1390)

Mann, C., Ferrand, K., Liu, S. et al. 2019. Influence of young cement water on the corrosion of the International Simple Glass. *npj Mater Degrad* v. 3, 5. DOI: 10.1038/s41529-018-0059-9

Mann, C., Thorpe, C., Milodowski, A.E. et al. 2017. Interactions between Simulant Vitrified Nuclear Wastes and high pH solutions: A Natural Analogue Approach. *MRS Advances* v. 2, p. 669–675. DOI: 10.1557/adv.2017.59

McMahon, W. J., & Davies, N. S. 2018. Evolution of alluvial mudrock forced by early land plants. *Science*, v. 359, p. 1022–1024. DOI: 10.1126/science.aan4660

Mills, B. J. W., Batterman, S. A. & Field, K. J. 2017. Nutrient acquisition by symbiotic fungi governs Palaeozoic climate transition. *Phil.Trans. R. Soc. B*, v. 373, 20160503.

Mansfield, J. 2022. Aqueous Dissolution of Nuclear Waste and Analogue Glasses: Dissolution Behaviour, Surface Layers and Vermiform Features. PhD Thesis, Department of Material Science and Engineering, The University of Sheffield.

McMahon, S., Cosmidis, J. 2021. False biosignatures on Mars: anticipating ambiguity. *Journal of the Geological Society*, v. 179 is. 2, jgs2021–050. DOI: 10.1144/jgs2021-050

Mcloughlin, N., Staudigel, H., Furnes, H., Eickmann, B. Ivarsson, M. 2010. Mechanisms of microtunneling in rock substrates: Distinguishing endolithic biosignatures from abiotic microtunnels. *Geobiology* v. 8, p. 245–255.

McLoughlin, N., Furnes, H., Banerjee, N. R., Muehlenbachs, K. & Staudigel, H. 2009.

Ichnotaxonomy of microbial trace fossils in volcanic glass. *J. Geol. Soc. London*. v. 166, p. 159–169.

Mitchell, R. L., Kenrick, P., Pressel, S., Duckett, J., Strullu-Derrien, C., Davies, N., McMahon, W. J., Summerfield, R. 2023. Terrestrial surface stabilization by modern analogues of the earliest land plants: A multi-dimensional imaging study. *Geobiology*, v. 21, p. 454-473. DOI: 10.1111/gbi.12546.

Mitchell, R. L., Strullu-Derrien, C., Sykes, D., Pressel, S., Duckett, J. G., Kenrick, P. 2021a. Cryptogamic ground covers as analogues for early terrestrial biospheres: Initiation and evolution of biologically mediated proto-soils. *Geobiology*. v. 193, p. 292-306. DOI: 10.1111/gbi.12431.

Mitchell, R.L., Davies, P., Kenrick, P. et al. 2021b. Correlative Microscopy: a tool for understanding soil weathering in modern analogues of early terrestrial biospheres. *Sci Reports*, v. 11, 12736. DOI: 10.1038/s41598-021-92184-1

Mitchell, R. L., Strullu-Derrien, C., Kenrick, P. 2019. Biologically mediated weathering in modern cryptogamic ground covers and the early Paleozoic fossil record. *Journal of the Geological Society*, v. 176, p. 430–439. DOI: 10.1144/jgs2018-191

Mitchell, R. L., Cuadros, J., Duckett, J. G., Pressel, S., Mavris, C., Sykes, D., Najorka, J., Edgecombe, G. D., Kenrick, P. 2016. Mineral weathering and soil development in the earliest land plant ecosystems. *Geology*, 44, 1007–1010. DOI: 10.1130/G38449.1

Morris, J. L., Puttick, M. N., Clark, J. W., Edwards, D., Kenrick, P., Pressel, S., Wellman, C. H., Yang, Z., Schneider, H., & Donoghue, P. C. J. 2018. The timescale of early land plant evolution. *Proceedings of the National Academy of Sciences*, 115(10), E2274–E2283. DOI: 10.1073/pnas.17195 88115

Puttick, M. N., Morris, J. L., Williams, T. A., Cox, C. J., Edwards, D., Kenrick, P., Pressel, S., Wellman, C. H., Schneider, H., Pisani, D., & Donoghue, P. C. J. 2018. The Interrelationships of Land Plants and the Nature of the Ancestral Embryophyte. *Current Biology*, 28, 733–745.e2.

Pinzari, F., Cuadros, J., Napoli, R., Canfora, L., Baussà Bardají, D. 2016. Routes of phlogopite weathering by three fungal strains. *Fungal Biol*; 120(12): 1582–1599. DOI: 10.1016/j.funbio.2016.08.007

Porada, P., Weber, B., Elbert, W., Pöschl, U., & Kleidon, A. 2014. Estimating impacts of lichens and bryophytes on global biogeochemical cycles. *Global Biogeochemical Cycles*, 28, 71–85. DOI: 10.1002/2013G B004705

Rosling, A., Lindahl, B D., Taylor, A F S., Finlay, R D. 2004. Mycelial growth and substrate acidification of ectomycorrhizal fungi in response to different minerals. *FEMS Microbiol Ecol*. 47(1), P. 31- 37. DOI: 10.1016/S0168-6496(03)00222-8.

Schmalenberger, A., Duran, A L., Bray, A W., Bridge, J., Bonneville, S., Benning, L G., et al. 2015. Oxalate secretion by ectomycorrhizal *Paxillus involutus* is mineral-specific and controls calcium 499 weathering from minerals. *Sci Reports*, v. 5, p. 1–14. DOI: 10.1038/srep12187

Steele, A., Benning, L. G., Wirth, R., Schreiber, A., Araki, T., McCubbin, F. M., Fries, M. D., Nittler, L. R., Wang, J., Hallis, L. J., Conrad, P. G., Conley, C., Vitale, S., O'Brian, A. C., Riggi, V., Rogers, K. 2022. Organic synthesis associated with serpentinization and carbonation on early Mars. *Science*, v. 375, Is. 6577, p. 172-177. DOI: 10.1126/science.abg7905.

Strother P. K, Foster C. 2021. A fossil record of land plant origins from charophyte algae. *Science*. V. 373, Is. 6556, p. 792-796. DOI: 10.1126/science.abj2927.

Thorseth, I. H., Torsvik, V. Torsvik, F.L. Daae, R.B. Pedersen. 2001. Diversity of life in ocean floor basalt. *Earth and Planetary Science Letters*, v. 194, Is. 1–2, p. 31-37. DOI: 10.1016/S0012-821X(01)00537-4.

Thorseth, I.H., Furnes, H., Tumyr, O. 1995. Textural and chemical effects of bacterial activity on basaltic glass: an experimental approach, *Chemical Geology*, v. 119, Is. 1–4, p. 139-160, DOI: 10.1016/0009-2541(94)00098-S.

Wacey, D., Kilburn, M., Stoakes, C., Aggleton, H. and Brasier, M. 2008. Ambient inclusion trails: their recognition, age range and applicability to early life on Earth. *Modern Approaches in Solid Earth Sciences*, v. 4, p. 113–134, DOI: 10.1007/978-1-4020-8306-8_3

Wild, B., Imfeld, G., Daval, D. 2021 Direct measurement of fungal contribution to silicate weathering rates in soil. *Geology*, v. 49, Is. 9, p. 1055–1058. DOI: 10.1130/G48706.1

Non-peer reviewed EarthArXiv preprint

van Schöll, L., Kuyper, T.W., Smits, M.M. et al. 2008. Rock-eating mycorrhizas: their role in plant nutrition and biogeochemical cycles. *Plant Soil*, v. 303, p. 35–47. DOI:

10.1007/s11104-007-9513-0

Zaharescu, D. G., Burghelea, C. I., Dontsova, K., Reinhard, C. T., Chorover, J., Lybrand, R.

2020. *Biogeochemical cycles*. V. 251, p. 3–32. DOI: 10.1002/9781119413332.ch1